Foxg1 regulates retinal axon pathfinding by repressing an ipsilateral program in nasal retina and by causing optic chiasm cells to exert a net axonal growth-promoting activity

Natasha M. Tian, Thomas Pratt and David J. Price*

Mammalian binocular vision relies on the divergence of retinal ganglion cell axons at the optic chiasm, with strictly controlled numbers projecting contralaterally and ipsilaterally. In mouse, contralateral projections arise from the entire retina, whereas ipsilateral projections arise from ventrotemporal retina. We investigate how development of these patterns of projection is regulated by the contralateral determinant Foxg1, a forkhead box transcription factor expressed in nasal retina and at the chiasm. In nasal retina, loss of Foxg1 causes increased numbers of ipsilateral projections and ectopic expression of the ipsilateral determinants *Zic2*, *Ephb1* and *Foxd1*, indicating that nasal retina is competent to express an ipsilateral program that is normally suppressed by Foxg1. Using co-cultures that combine Foxg1-expressing with *Foxg1*-null retinal explants and chiasm cells, we provide functional evidence that Foxg1 promotes contralateral projections through actions in nasal retina, and that in chiasm cells, Foxg1 is required for the generation of a hitherto unrecognized activity supporting RGC axon growth.

KEY WORDS: Foxg1, Retinal ganglion cell, Chiasm, Mouse

INTRODUCTION

Binocular vision in mammals is possible because some retinal ganglion cell (RGC) axons project to the same side of the brain (ipsilaterally), whereas others project to the opposite side (contralaterally). This allows signals from RGCs activated by a single visual stimulus simultaneously in the two eyes to converge in the brain for processing. During embryonic development, RGC axons extend along the optic nerves to reach the brain's ventral midline, where they either turn away from the midline to project ipsilaterally or continue contralaterally at the optic chiasm.

The optic chiasm begins forming around embryonic day 12 (E12) in mouse, shortly after the initiation of RGC genesis. At first, RGCs in dorsocentral retina project pioneering contralateral axons and a smaller number of transient ipsilateral axons (Colello and Guillery, 1990; Guillery et al., 1995; Insausti et al., 1984; Marcus et al., 1995; Mason and Sretavan, 1997). The peak phase of RGC genesis and RGC axon growth through the chiasm occurs at E14-16, when the permanent ipsilateral projection forms (Colello and Guillery, 1990). Contralateral RGC axons arise from the entire retina, whereas permanent ipsilateral RGC axons arise mainly from the ventrotemporal crescent (VTC), a small region of peripheral ventrotemporal (VT) retina. The adult pattern of decussation is established by birth with a 95-97% to 3-5% ratio of contralateral to ipsilateral axons (Drager and Olsen, 1980; Drager, 1985).

In vitro and in vivo experiments have demonstrated that ipsilateral-contralateral divergence at the chiasm involves repulsive factors acting at or around the chiasm (reviewed by Erskine and Herrera, 2007). During the peak period of retinal axon divergence, the mouse optic chiasm expresses molecules inhibitory to axon growth, including ephrin B2 (Nakagawa et al., 2000; Williams et al., 2003), heparan sulphate proteoglycan modifying enzymes (Pratt et

al., 2006), chondroitin sulphate proteoglycans (Chung et al., 2000a; Chung et al., 2000b; Tuttle et al., 1998), CD44 (Sretavan et al., 1994; Sretavan et al., 1995), stage-specific embryonic antigen 1 (Marcus and Mason, 1995; Sretavan et al., 1994) (SSEA-1) and slit proteins (Erskine et al., 2000; Niclou et al., 2000; Plump et al., 2002; Ringstedt et al., 2000; Thompson et al., 2006a; Thompson et al., 2006b). Most of these reduce axon growth from all retinal regions, rather than VT axons selectively. Ephrin B2, however, which is expressed by midline radial glia, is necessary and sufficient for the repulsion of EphB1-bearing VT axons into the ipsilateral optic tract (Williams et al., 2003). By contrast, contralateral axons do not express EphB1 during the peak phase of ipsilateral projections and so their axons are not repelled by ephrin B2 at the chiasm. To date, there is no evidence for an attractive factor in developing mouse ventral diencephalon promoting growth of contralateral but not ipsilateral axons across the chiasm.

Recent work has identified transcription factors that regulate the expression of key RGC axon guidance molecules (reviewed by Erskine and Herrera, 2007). A notable example of an ipsilateral determinant is the zinc-finger transcription factor Zic2, which is expressed by RGCs in the VTC, is sufficient for their axons to project ipsilaterally and is thought to act via transcriptional regulation of their EphB1 axon guidance receptor levels (Herrera et al., 2003; Williams et al., 2003; Lee et al., 2008; Garcia-Frigola et al., 2008). A transcription factor implicated in promoting the contralateral projection of RGC axons is Foxg1, a winged helix transcription factor expressed by nasal RGCs, nasal optic stalk and presumptive optic chiasm (Hatini et al., 1994; Huh et al., 1999; Pratt et al., 2004). *Foxg1*$^{-/-}$ mouse embryos show a significant increase in the number of ipsilateral projections (Pratt et al., 2004); strikingly, they develop a major ipsilateral projection from nasal retina.

Here, we have investigated the mechanism of action of Foxg1 in determining the laterality of RGC axon projections. We found a significant increase in the number of Zic2-expressing RGCs and ectopic *Ephb1* expression in *Foxg1*$^{-/-}$ DN retina. We used an in vitro assay to test whether Foxg1 is required by nasal RGCs, by comparing axon growth from *Foxg1*-expressing and *Foxg1*$^{-/-}$ dorsonasal (DN)

Centre for Integrative Physiology, The University of Edinburgh, Hugh Robson Building, George Square, Edinburgh EH8 9XD, UK.

*Author for correspondence (e-mail: david.price@ed.ac.uk)

retinal explants co-cultured with dissociated chiasm cells from *Foxg1*-expressing embryos. This co-culture approach has an established track record in demonstrating differential responses of different types of RGCs to chiasm cells: for example, wild-type VT retinal axons grow less well than wild-type DN retinal axons on chiasm cells, reflecting the fact that many VT retinal axons are repelled from the chiasm into the ipsilateral optic tract in vivo (Herrera et al., 2003; Herrera et al., 2004; Marcus et al., 1995; Marcus and Mason, 1995; Marcus et al., 1996; Wang et al., 1995). We found that Foxg1 is required in DN retina for its axons to grow normally on chiasm cells. We also tested whether Foxg1 is required by chiasm cells, by comparing axon growth from *Foxg1*-expressing DN or VT retina co-cultured with dissociated chiasm cells from either *Foxg1*-expressing or *Foxg1⁻/⁻* embryos. These experiments indicated that Foxg1 is also required at the optic chiasm for its cells to support the normal growth of retinal axons.

MATERIALS AND METHODS

Animals

The *Foxg1^{LacZ}* allele (CBA) (Xuan et al., 1995) enables identification of cells in which the *Foxg1* locus is transcriptionally active. Co-cultures used pigmented mouse embryos from *Foxg1^{LacZ/+}* (CBA) and *Foxg1^{Cre/+}* (Swiss Webster) matings. The Foxg1-coding sequences in the *Foxg1^{Cre}* allele are replaced by a Cre recombinase cassette (Hebert and McConnell, 2000). *Foxg1^{LacZ}* and *Foxg1^{Cre}* are predicted null alleles (Hebert and McConnell, 2000; Xuan et al., 1995).

PCR genotyping *Foxg1* alleles

Foxg1^{LacZ/LacZ} and *Foxg1^{Cre/Cre}* embryos were identified by their severely hypoplastic telencephalon and eye deformities. *Foxg1^{LacZ/+}* embryos were distinguished from *Foxg1^{+/+}* embryos by PCR of embryonic tails using primers *lacZ* F2 (5′-TTG AAC TGC CTG AAC TAC CG-3′) and *lacZ* R2 (5′-CCT GAC TGG CGG TTA AAT TG-3′). Cycling conditions were as previously described (Pratt et al., 2004).

Histochemistry

Embryos were fixed in 4% paraformaldehyde (PFA) in phosphate-buffered saline (PBS) for 2 hours. *lacZ* staining on cryostat sections (10 μm) or whole mounts and immunohistochemistry on cryostat sections (10 μm) or wax sections (10 μm) were performed as previously described (Pratt et al., 2004). Primary antibodies were: rabbit polyclonal Zic2 antibody (1/8,000) (Stephen Brown, Columbia University, New York (Brown et al., 2003); mouse monoclonal Brn3a antibody (1/300) (Chemicon International). Fluorescent secondary detection used goat anti-rabbit IgG AlexaFluor 488 and goat anti-mouse IgG AlexaFluor 546 antibodies (1/150; Molecular Probes) and sections were counterstained using TO-PRO-3 (1/2,000; Molecular Probes). Non-fluorescent detection of Zic2 or Brn3a was via a diaminobenzidine (DAB) colour reaction (Zic2: Rabbit Envision+ kit, Dako K4010; Brn3a: mouse Envision+ kit, Dako K4006).

For each eye, numbers of labelled cells were counted in six evenly spaced sections from dorsal to ventral: the dorsal- and ventral-most sections in which Brn3a-positive cells were visible were identified and the intervening four sections were then chosen by dividing up the distance between the dorsal- and ventral-most sections equally. One-way ANOVA was used to assess the significance of differences between groups and, where differences were significant ($P<0.05$), two-tailed Student's *t*-tests assuming equal variances were used to assess differences between pairs of groups.

Co-cultures

Retinal explants were cultured in collagen gels surrounded by dissociated chiasm cells of the same age (E14.5). Co-cultures were prepared based on a method described previously (Wang et al., 1996). Collagen (10-20 μl) was spread evenly onto circular glass coverslips and allowed to set at 37°C. Equal-sized retinal explants from peripheral DN or VT retina (regions shown in Fig. 1C) were placed on top of the collagen in 20 μl of serum-free culture medium containing 0.5% methylcellulose to aid adhesion. Explants were incubated at 37°C for 2 hours, allowing them to adhere to the collagen gel. Tissue that would provide optic chiasm cells was cut from the ventral surface of the brain

and included a region extending ~200 μm anterior, posterior and lateral to the decussation so as to include the *Foxg1*-expressing region. Chiasm tissue was dissociated using papain (Worthington Biochemical Corporation, #LK003160) and cells were resuspended in a 1:1 mixture of rat-tail and bovine collagen before being added to the retinal explants at 50,000 cells/mm². After 2 hours, fresh serum-free culture medium without methylcellulose was added to the cultures, which were then incubated at 37°C for 48 hours. Co-cultures were fixed in 4% PFA in PBS after 48 hours followed by neurofilament and Brn3a immunohistochemistry. The co-cultures were blocked in 10% goat serum, 0.2% Triton-X-100 in PBS (PBSTx-100) for 90 minutes at room temperature prior to overnight incubation at 4°C with primary antibodies: rabbit neurofilament (1/200) (Biomol International) and mouse Brn3a (1/300) (Chemicon International). Following washes in 0.1% PBSTx-100 at room temperature, the cultures were incubated overnight at 4°C with secondary antibodies: goat anti-mouse Alexa Fluor 546 (1/500) (Molecular Probes) and goat-anti-rabbit Alexa Fluor 488 (1/500) (Molecular Probes). Following 0.1% PBSTx-100 washes, cultures were incubated in TO-PRO-3 (1/2,000) for 1 hour and mounted in a 9:1 solution of glycerol: PBS. The densities of chiasm cells that were viable, judged by high-power examination of nuclei after culture, were counted in three sampling boxes adjacent to the explant border: mean densities were 28,000-38,000 cells/mm² and did not vary significantly between any of the different co-culture combinations by ANOVA ($P=0.653$) (see Fig. S1 in the supplementary material). Neurite outgrowth was quantified for all retinal explants by obtaining measures of its amount and length (see Fig. S2 in the supplementary material). The amount of outgrowth was estimated by surrounding each explant by a line at 23, 45, 68 or 91 μm from its edge [e.g. yellow polygon in Fig. S2B (see supplementary material) 45 μm from edge] and calculating the percentage of its circumference that was covered by neurites crossing it (see Fig. S2C,D in the supplementary material). This estimate is referred to as 'percentage axon coverage'. A measure of length was obtained by calculating the mean of the lengths of the five longest neurites for each culture. One-way ANOVA was used to assess the significance of differences between groups and, where differences were significant ($P<0.05$), Tukey tests were used to assess differences between pairs of groups (*n* values stated in Results are numbers of explants).

Ephb1 and *Foxd1* in situ hybridization

Digoxigenin-labelled antisense riboprobes were from mouse *Ephb1* and *Foxd1* cDNAs. *Ephb1* in situ hybridization was on 10 μm paraffin sections (Christoffels et al., 2000). Foxd1 in situ hybridization was on 100 μm vibrotome sections (Erskine et al., 2000).

RESULTS

Foxg1 is expressed in DN retina

To characterize retinal *Foxg1* expression throughout the period when retinal axons navigate the optic chiasm, serial horizontal sections from E13.5-15.5 *Foxg1^{LacZ/+}* embryos (Fig. 1) were reacted to reveal *lacZ* expression [E13.5-15.5 *Foxg1^{LacZ/+}* embryos did not display noticeable morphological defects in the eyes or forebrain, confirming previous reports (Huh et al., 1999; Pratt et al., 2004; Xuan et al., 1995)]. Dorsal retina showed widespread *lacZ* staining (Fig. 1E). Moving ventrally, *lacZ* staining retreated progressively nasally (Fig. 1F-J), until it was absent from the entire retina in extremely ventral sections (Fig. 1K). A diagram of *Foxg1* activation deduced from these data in the E14.5 retina is shown in Fig. 1B (results were the same at E13.5 and E15.5; not shown). The border between *Foxg1*-positive and *Foxg1*-negative regions runs at an angle to the dorsoventral axis, such that *Foxg1* is expressed in DN regions, declining towards the VT retina, where *Foxg1* expression is entirely absent.

Zic2, *Ephb1* and *Foxd1* expression are altered in the *Foxg1⁻/⁻* nasal retina

The *Foxg1⁻/⁻* retina produces an increased ipsilateral projection, much of which arises ectopically from nasal retina. Previous work has shown that at E14.5-16.5, when VTC axons are navigating
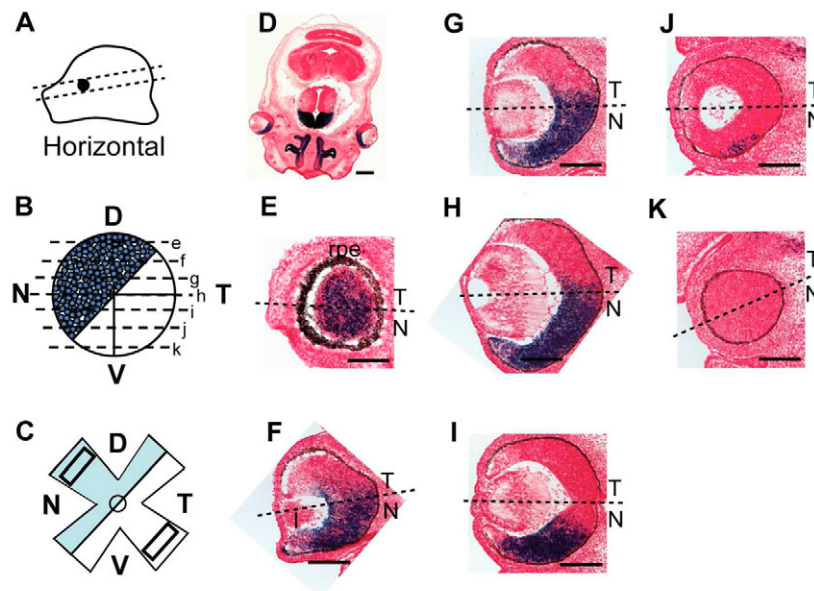
Fig. 1. Transcriptional activation of *Foxg1* in the retina at E14.5. X-gal staining (blue) of *Foxg1*^(LacZ/+) embryos is used to show where *Foxg1* is active. (**A**) Schematic of a mouse embryo head showing the horizontal plane of section; broken lines indicate the limits between which sections were taken. (**B**) Schematic of retina showing the locations of sections in E-K; blue circles indicate *Foxg1*-expressing RGCs. (**C**) Diagram of a flat-mounted retina, with blue shading indicating the area of transcriptional activation of *Foxg1*; boxed areas indicate regions from which DN (*Foxg1*-positive) and VT (*Foxg1*-negative) retinal explants were prepared for the co-culture experiments. (**D**) A *Foxg1*^(LacZ/+) embryo showing X-gal staining mainly in nasal retinae. (E-K) Dorsal to ventral series of sections (locations marked in B) through a retina shown in D counterstained with Nuclear Fast Red (pink). (**E**) At the dorsal pole, X-gal staining is found throughout all layers of nasal and temporal retina. (**F-H**) Moving from dorsal to central sections, X-gal staining is present throughout nasal retina and occupies progressively less of temporal retina. (**I-K**) Moving through ventral sections, the X-gal-stained part of nasal retina becomes smaller and increasingly restricted to the anterior-most region of nasal retina until it disappears in the most ventral section. Scale bars: 500 µm in D; 200 µm in E-K. Abbreviations: D, dorsal; N, nasal; T, temporal; V, ventral; l, lens; rpe, retinal pigment epithelium. Broken lines in E-K indicate nasal-temporal boundary.

ipsilaterally, the zinc-finger transcription factor Zic2 and the axon guidance receptor EphB1 determine the navigation of ipsilaterally projecting RGC axons from the VTC (Herrera et al., 2003; Williams et al., 2003). Here, we have considered the possibility that in the absence of Foxg1 these ipsilateral determinants are upregulated in nasal retina.

Immunohistochemistry was used to visualize the location of Zic2- and Brn3a-expressing RGCs in the retina of E14.5 and E16.5 *Foxg1*^(+/+) and *Foxg1*^(–/–) embryos (Fig. 2). Some Zic2-expressing cells were observed peripheral to the most peripheral Brn3a-expressing RGCs, indicating that Zic2 is expressed in newly differentiated RGCs prior to expression of Brn3a, in agreement with previous findings (Herrera et al., 2003).

In E14.5 *Foxg1*^(+/+) retina (Fig. 2A-H), Zic2-expressing cells were predominantly in VT retina, with strongest expression in a cluster in the RGC layer adjacent to the strongly Zic2-expressing ciliary marginal zone (CMZ) (Fig. 2C,D,G), as described before (Herrera et al., 2003). In other regions of *Foxg1*^(+/+) retina, weak staining for Zic2 was seen in small numbers of cells in the RGC layer, although most Zic2-positive cells were outside the RGC layer and were Brn3a negative (Fig. 2E,F,H). Quantification of all cells staining positive for Zic2 in the RGC layer (irrespective of their level of staining) in six evenly spaced horizontal sections (Fig. 3A), is shown in Fig. 3B,C (light blue bars show *Foxg1*^(+/+) data): in *Foxg1*^(+/+) embryos, there were more Zic2-expressing cells in VT retina than in other quadrants, as described previously (Herrera et al., 2003).

In E14.5 *Foxg1*^(–/–) retina (Fig. 2I-P), Zic2 is still expressed in the RGC layer of VT retina (Fig. 2L,P) and quantification in this region revealed no significant difference in proportions of Zic2-positive cells

compared with those in *Foxg1*^(+/+) embryos at E14.5 and E16.5 (right-hand bars in Fig. 3B,C). However, large increases in the proportion of Zic2-expressing cells were visible in the RGC layer of DN (Fig. 2J,N) and ventronasal (VN) (Fig. 2K,O) retina. Quantification in *Foxg1*^(+/+) and *Foxg1*^(–/–) DN and VN retina confirmed that there were significantly greater proportions of Zic2-expressing cells in *Foxg1*^(–/–) nasal retina (Fig. 3B,C). Quantification of numbers of Brn3a-expressing RGCs at E14.5 and E16.5 revealed no significant differences between *Foxg1*^(+/+) and *Foxg1*^(–/–) retinae, ruling out the possibility that changes in numbers of RGCs account for increased Zic2 expression (see Fig. S3 in the supplementary material).

To investigate whether ectopic expression of Zic2 was associated with ectopic *Ephb1* expression in *Foxg1*^(–/–) nasal retina, the distribution of *Ephb1* mRNA was revealed using in situ hybridization (Fig. 4). In *Foxg1*^(+/+) embryos, strong staining for *Ephb1* was observed in RGCs in the VTC (Fig. 4B,C), in agreement with previous reports (Williams et al., 2003). In *Foxg1*^(–/–) mutants, *Ephb1*-expressing RGCs were observed in VT retina, as in *Foxg1*^(+/+) embryos (Fig. 4F,H). High levels of *Ephb1* expression were also observed in clusters of nasal RGCs (Fig. 4D-G, arrows in D,F, box in E) the distributions of which matched those of Zic2-expressing RGCs in mutant nasal retina.

Previous studies have shown that loss of the transcription factor Foxd1, the expression of which is complementary to that of Foxg1 in normal retina, results in loss of Zic2 and EphB1 from the VTC, suggesting that Foxd1 might be an upstream activator of Zic2 and *Ephb1* (Herrera et al., 2004). We used in situ hybridization to test whether *Foxd1* expression expands into DN retina. Sections from *Foxg1*^(+/+) embryos confirmed the expected expression of *Foxd1* in temporal retina (Fig. 4I-K). In *Foxg1*^(–/–) mutants, *Foxd1* was
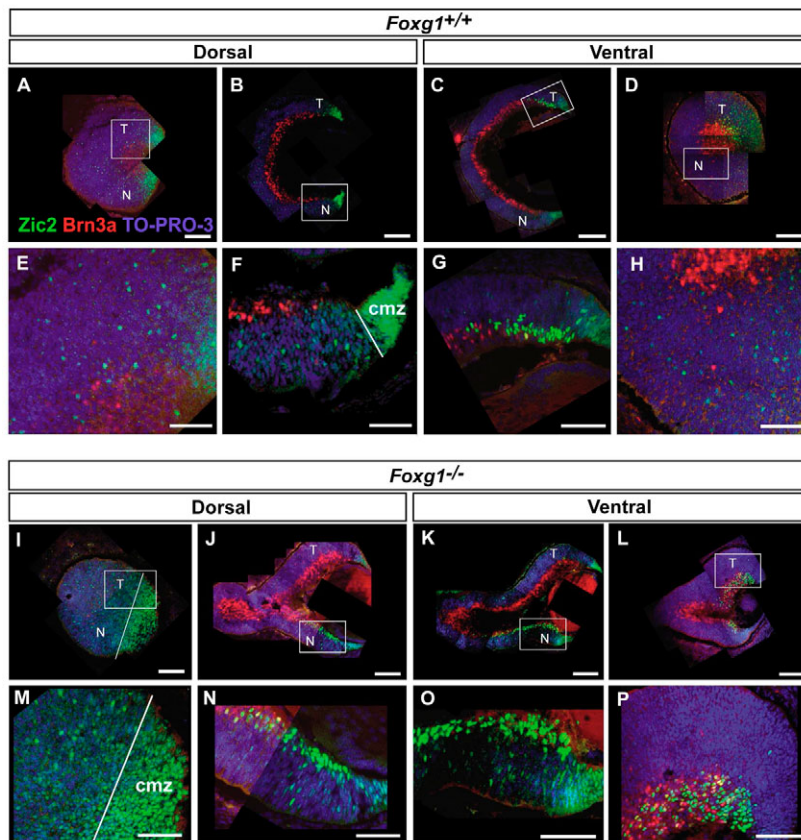
Fig. 2. Zic2 is expressed ectopically in nasal retina of *Foxg1*^{−/−} embryos. Zic2 (green) and Brn3a (red) immunohistochemistry in (A-H) wild-type and (I-P) *Foxg1*^{−/−} retinas at E14.5. (E-H) Higher magnifications of boxed areas in A-D, respectively. (M-P) Higher magnifications of boxed areas in I-L, respectively. (**A,B,E,F**) In wild-type dorsal retina, there are few Zic2-expressing cells in the inner retinal (RGC) layer; some are seen in other layers and there is strong expression in CMZ (marked in F), as reported previously (Herrera et al., 2003). (**C,D,G,H**), Zic2-expressing inner retinal layer cells are found predominantly in VT retina clustered adjacent to the CMZ (in boxed area in C). (**I,J,M,N**) In *Foxg1*^{−/−} dorsal retina; numerous Zic2-expressing cells are seen nasally, adjacent to the CMZ in the inner retinal layer (boxed area in J). (**K,L,O,P**) In *Foxg1*^{−/−} ventral retina; Zic2-expressing inner retinal layer cells are seen both nasally and temporally (boxed areas in K and L). Abbreviations: N, nasal; T, temporal; cmz, ciliary marginal zone. Scale bars: 200 µm in A-D,I-L; 100 µm in E-H,M-P.

expressed more widely in both temporal and nasal retina (Fig. 4L-N). In ventral sections, staining for *Foxd1* expression was strongest temporally (Fig. 4N), but in more dorsal sections there was very strong ectopic nasal expression (Fig. 4L,M).

Evidence from in vitro assays that Foxg1 is required in both DN retina and at the chiasm for appropriate RGC axon growth

To assay the functional importance of Foxg1 in the retina and test whether defects of chiasm cells might contribute to axon guidance defects in *Foxg1*^{−/−} embryos, DN and VT retinal explants from E14.5 *Foxg1*-expressing or *Foxg1*^{−/−} mouse embryos were cultured: (1) on their own, to determine the effect of Foxg1 on axon growth in the absence of chiasm cells; and (2) with *Foxg1*-expressing or

Foxg1^{−/−} dissociated chiasm cells. At E14.5, *Foxg1*^{LacZ/+} embryos are indistinguishable morphologically from *Foxg1*^{+/+} embryos (Huh et al., 1999; Pratt et al., 2004; Xuan et al., 1995) and do not show abnormal proportions of ipsilateral projections (Pratt et al., 2004) (N.M.T., T.P. and D.J.P., unpublished). For this reason, and to avoid the need to genotype embryos prior to culture (whereas E14.5 *Foxg1*^{−/−} embryos are easily recognized morphologically, genotyping is required to distinguish *Foxg1*^{+/−} from *Foxg1*^{+/+} embryos), both genotypes were used to provide *Foxg1*-expressing tissue that is referred to here as *Foxg1*^{+/±}. The DN retinal explants were dissected from the centre of the region that normally expresses *Foxg1*, whereas the VT explants were dissected from *Foxg1*-negative retina, as shown in Fig. 1C. Explants were dissected from equivalent regions in *Foxg1*^{+/±} and *Foxg1*^{−/−} retinae.
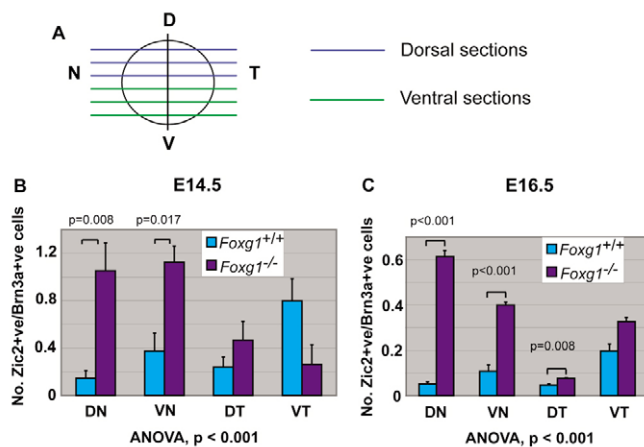
Fig. 3. Increased proportion of Zic2-expressing cells in nasal retina of *Foxg1*^{−/−} embryos at E14.5 and E16.5. (**A**) For each retina, numbers of nasal and temporal Zic2-positive and Brn3a-positive cells were counted in six sections spaced at 80-100 µm intervals through the retina from dorsal (blue horizontal lines) to ventral (green horizontal lines). (**B,C**) Means (±s.e.m.) are counts of Zic2-positive cells expressed as a proportion of numbers of Brn3a-positive cells in the four retinal quadrants. At E14.5 and E16.5, *Foxg1*^{−/−} nasal quadrants showed large significant increases in the proportion of Zic2-positive cells compared with equivalent wild-type quadrants. No significant differences were found between proportions of Zic2-positive cells in *Foxg1*^{−/−} and wild-type VT retina at both ages. Brackets indicate significant differences, with *P* values indicated above each bracket. Numbers of retinae: *Foxg1*^{+/+}, n=4; *Foxg1*^{−/−}, n=3. Abbreviations: DN, dorsonasal; VN, ventronasal; DT, dorsotemporal; VT, ventrotemporal.
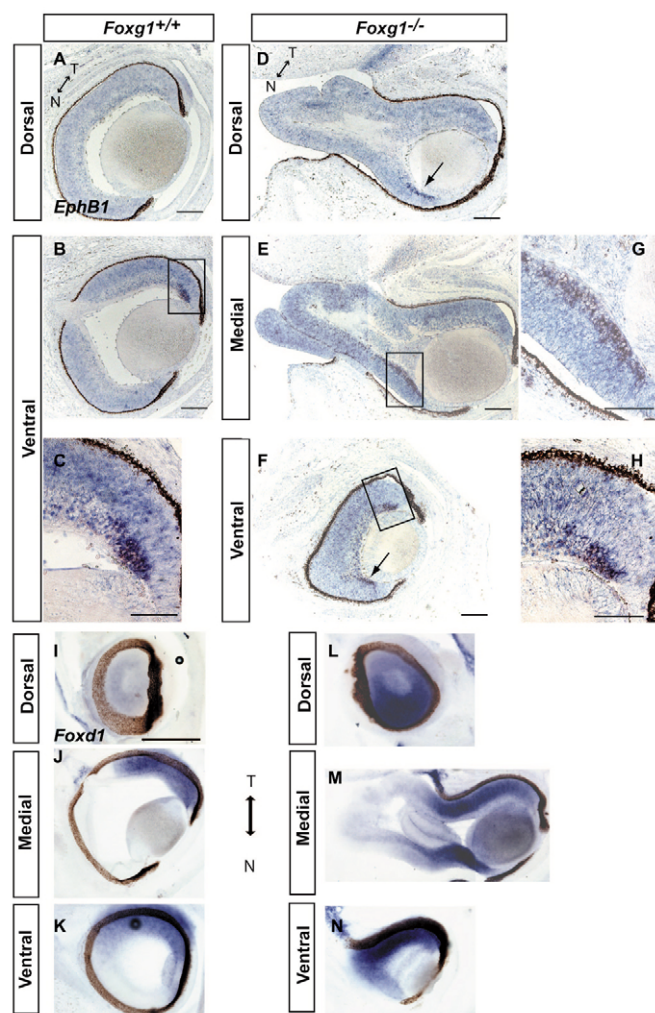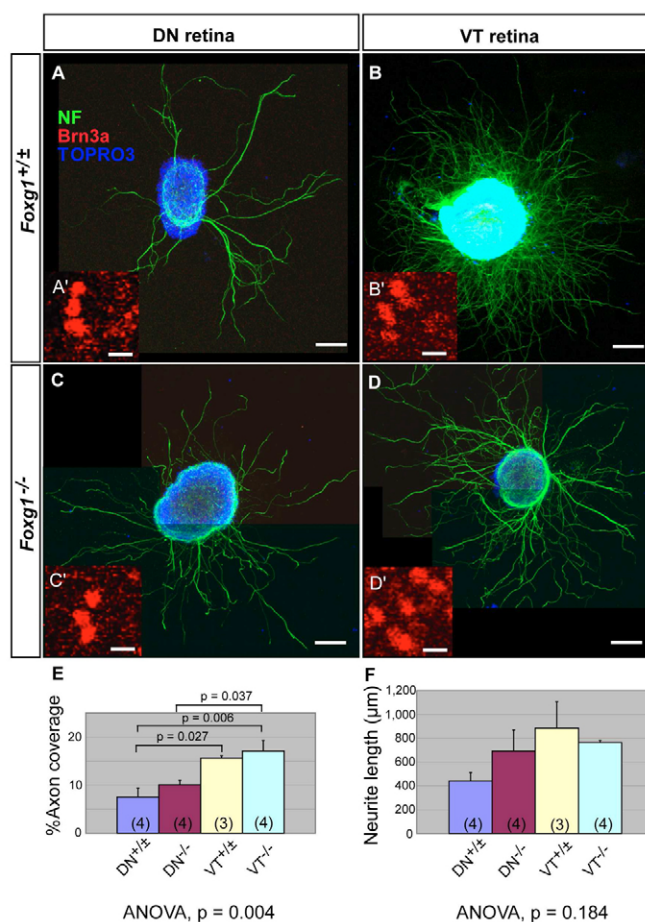
Fig. 4. *Ephb1* and Foxd1 are expressed ectopically in the nasal retina of *Foxg1⁻/⁻* embryos. (**A-H**) *Ephb1* in situ hybridization in (A-C) wild-type and (D-H) *Foxg1⁻/⁻* retinas at E16.5; C,G,H show higher magnifications of boxed areas in B,E,F, respectively. In wild-type and in *Foxg1⁻/⁻* retinas, *Ephb1* is expressed in peripheral VT RGCs (B,C,F,H). In *Foxg1⁻/⁻* retinas, *Ephb1* is expressed ectopically in the nasal retina in (D) dorsal, (E,G) medial and (F,H) ventral sections (indicated by arrows in D, F and boxed area in E). (**I-N**) *Foxd1* in situ hybridization in (I-K) wild-type and (L-N) *Foxg1⁻/⁻* retinas at E16.5. In *Foxg1⁻/⁻* retinas, Foxd1 is expressed ectopically in DN retina. Temporal is towards the top of all panels. Scale bars: 200 µm in A,B,D-F; 100 µm in C,G,H; 400 µm in I-N.

Fig. 5. *Foxg1* is not required for retinal outgrowth in culture. (A) DN *Foxg1⁺/±*, (B) VT *Foxg1⁺/±*, (C) DN *Foxg1⁻/⁻* and (D) VT *Foxg1⁻/⁻* retinal explants cultured in collagen without chiasm cells. (**A-D**) Neurofilament (NF) immunohistochemistry revealed neurite outgrowth from all explants. (**A'-D'**) Brn3a expression in co-cultures A-D respectively revealed healthy RGCs. (**E**) Mean percentage axon coverage (±s.e.m.) for *Foxg1⁺/±* and *Foxg1⁻/⁻* retinal explants from DN and VT retina 45 µm from the retinal explant (measured as in Fig. S2 in the supplementary material). (**F**) Mean length of the longest neurites (±s.e.m.) for each set of explants. (E,F) Numbers of explants are indicated in parentheses. (E) One-way ANOVA showed a significant effect of explant type; significant differences are marked by brackets with *P* values indicated. (F) One-way ANOVA revealed no significant differences in the lengths of outgrowth among retinal explants. Abbreviations: DN, dorsonasal; VT, ventrotemporal. Scale bars: 100 µm in A-D; 10 µm in A'-D'.

Retinal axon outgrowth in the absence of chiasm cells

To investigate whether intrinsic growth differences exist between *Foxg1⁺/±* and *Foxg1⁻/⁻* RGC axons, retinal explants were cultured alone without chiasm cells. Fig. 5A-D shows typical confocal images of *Foxg1⁺/±* and *Foxg1⁻/⁻* explants from DN and VT retina. Fluorescence immunohistochemistry reveals expression of the axon marker neurofilament (green) and the POU-homeodomain transcription factor Brn3a (red), expressed by postmitotic RGCs (Pan et al., 2005). Brn3a-expressing RGCs were present and appeared healthy in all retinal explants.

The amount of outgrowth from explants in collagen gel cultures (mean percentage axon coverage) was significantly greater from VT *Foxg1⁺/±* retinal explants than from DN *Foxg1⁺/±* retinal

explants (Fig. 5E), in agreement with previous observations (Wang et al., 1996), demonstrating that axons from the VT retina, many of which normally project ipsilaterally at the chiasm, are capable of prolific growth in the absence of chiasm cells. This was also true for DN *Foxg1⁻/⁻* retina versus VT *Foxg1⁻/⁻* retina. Importantly, we found no significant differences in the amounts of outgrowth or the lengths of the longest neurites between *Foxg1⁺/±* and *Foxg1⁻/⁻* DN or *Foxg1⁺/±* and *Foxg1⁻/⁻* VT explants (Fig. 5E,F). In view of these results, differences in the growth of axons from *Foxg1⁺/±* and *Foxg1⁻/⁻* DN explants or from *Foxg1⁺/±* and *Foxg1⁻/⁻* VT explants in the presence of *Foxg1⁺/±* or *Foxg1⁻/⁻* chiasm cells described in the following sections can be attributed to differences in the interaction of these explants with chiasm cells.

DN retinal axon outgrowth on chiasm cells

Co-cultures were prepared in the following combinations: (1) DN *Foxg1*[+/±] retina with *Foxg1*[+/±] chiasm cells; (2) DN *Foxg1*^{−/−} retina with *Foxg1*[+/±] chiasm cells; (3) DN *Foxg1*[+/±] retina with *Foxg1*^{−/−} chiasm cells; (4) DN *Foxg1*^{−/−} retina with *Foxg1*^{−/−} chiasm cells (compositions of co-cultures will be notated as *Foxg1*[+/±] retina ↔ *Foxg1*[+/±] chiasm, *Foxg1*^{−/−} retina ↔ *Foxg1*[+/±] chiasm, etc.).

Fig. 6A shows a typical confocal image of a DN *Foxg1*[+/±] retina ↔ *Foxg1*[+/±] chiasm co-culture. Prolific neurite growth was seen from all sides of the explant, reaching far into the surrounding chiasm cells. By contrast, DN *Foxg1*^{−/−} retina ↔ *Foxg1*^{−/−} chiasm co-cultures consistently displayed limited neurite growth into the surrounding chiasm cells: neurites were short and highly fasciculated, and a large proportion wrapped around the explant (Fig. 6D). DN *Foxg1*^{−/−} retina ↔ *Foxg1*^{−/−} chiasm co-cultures showed a significantly lower percentage of axon coverage and shorter neurite lengths than did DN *Foxg1*[+/±] retina ↔ *Foxg1*[+/±] chiasm co-cultures (Fig. 6E,F, compare 1st and 4th bars). This in vitro result reflects the increased avoidance of the *Foxg1*^{−/−} chiasm by nasal *Foxg1*^{−/−} retinal axons in *Foxg1*^{−/−} embryos in vivo (Pratt et al., 2004).

Culturing *Foxg1*[+/±] retina with *Foxg1*^{−/−} chiasm cells, or *Foxg1*^{−/−} retina with *Foxg1*[+/±] chiasm cells, enabled us to investigate the effect on retinal axon growth of removing *Foxg1* from chiasm cells or from the retina. Fig. 6B shows an example of a typical DN *Foxg1*[+/±] retina ↔ *Foxg1*^{−/−} chiasm co-culture. In comparison with the DN *Foxg1*[+/±] retina ↔ *Foxg1*[+/±] chiasm co-culture shown in Fig. 6A, fewer and shorter neurites were observed. This is reflected in a significant reduction in percentage axon coverage and mean neurite length (Fig. 6E,F, compare 1st and 3rd bars). In addition, DN *Foxg1*^{−/−} retina ↔ *Foxg1*^{−/−} chiasm co-cultures had significantly lower mean percentage axon coverage compared with DN *Foxg1*^{−/−} retina ↔ *Foxg1*[+/±] chiasm co-cultures (Fig. 6E, compare 2nd and 4th bars). These results indicate that loss of Foxg1 from chiasm cells reduces their ability to support retinal axonal growth.

Our data indicate that DN axons grow better in the presence of chiasm cells than in their absence (mean percentage axon coverage and lengths of longest neurites were roughly double in the presence of chiasm cells) (Fig. 5E,F and Fig. 6E,F, compare 1st bars). Loss of Foxg1 from chiasm cells reduces the growth of Foxg1-expressing DN axons to levels below those seen from Foxg1-expressing DN axons grown in the absence of chiasm cells (compare 1st bars in Fig. 5E,F with 3rd bars in Fig. 6E,F). This suggests that chiasm cells might normally play an active Foxg1-dependent role in supporting the growth of DN axons, and that the loss of Foxg1 from the chiasm converts this positive role to an inhibitory one.

The effect of removing *Foxg1* from DN retina can be seen in Fig. 6C, which shows a typical DN *Foxg1*^{−/−} retina ↔ *Foxg1*[+/±] chiasm co-culture. Fewer neurites were seen compared with DN *Foxg1*[+/±] retina ↔ *Foxg1*[+/±] chiasm co-cultures. Quantification showed a significant reduction in percentage axon coverage (Fig. 6E, compare 1st and 2nd bars) although there was no significant reduction in the lengths of the longest neurites (Fig. 6F, compare 1st and 2nd bars). Amounts of outgrowth from *Foxg1*^{−/−} DN retina cultured with *Foxg1*[+/±] chiasm cells remained similar to those from *Foxg1*^{−/−} DN retinal explants cultured without chiasm cells (compare 2nd bars in Fig. 5E,F with 2nd bars in Fig. 6E,F).

Data presented above are for measurements at 45 µm from the explant. Data on percentage axon coverage at other distances, from 23 µm to 91 µm, are shown in Fig. S4 in the supplementary material. Predictably, average percentage axon coverage fell as the distance
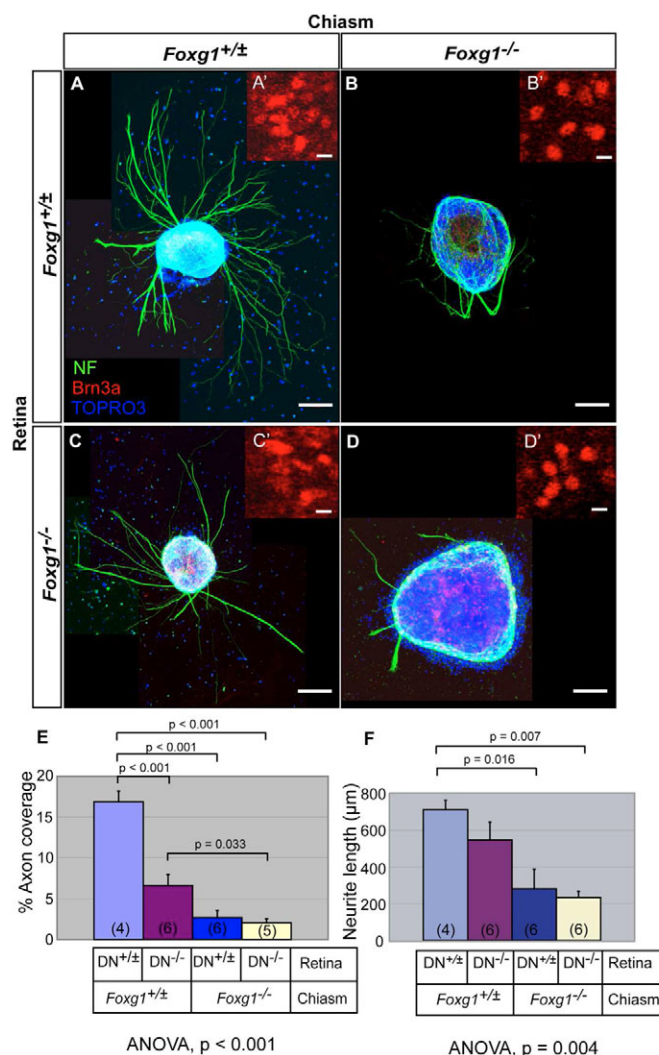
Fig. 6. Loss of Foxg1 from retina or chiasm impairs outgrowth of dorsonasal retinal axons on chiasm cells in culture. (**A-D**) Co-cultures of *Foxg1*[+/±] or *Foxg1*^{−/−} dorsonasal (DN) retinal explants with dissociated *Foxg1*[+/±] or *Foxg1*^{−/−} chiasm cells; immunohistochemistry is for the axonal marker neurofilament (NF; green) and the RGC marker Brn3a (red); the nuclear counterstain TO-PRO-3 (blue) reveals cells in the retinal explant and surrounding dissociated chiasm cells. Cultures in A and C are shown at half the magnification of those in B and D. (**A'-D'**) Brn3a expression in co-cultures A-D, respectively. (**E**) Mean percentage axon coverage (±s.e.m.) 45 µm from the retinal explant, showing significant differences among the four combinations. (**F**) Mean lengths of the five longest neurites (± s.e.m.). (E,F) Numbers of explants are in parentheses. One-way ANOVA revealed significant differences in outgrowth among retinal explants. Significant differences with *P* values are indicated above each bracket. Scale bars: 200 µm in A,C; 100 µm in B,D; 10 µm in A'-D'.

from the retinal explant increased, but the differences between the different types of co-culture remained the same at each point of measurement.

In summary, our data provide functional evidence that Foxg1 is required in its normal region of expression in the DN retina to support the growth of DN RGC axons across chiasm cells: whereas the addition of *Foxg1*[+/±] chiasm cells enhanced outgrowth from *Foxg1*[+/±] DN retina in culture, addition of *Foxg1*[+/±] chiasm did not have this effect on *Foxg1*^{−/−} DN retina. This is likely to be explained

by changes in expression of Zic2 and Ephb1 in *Foxg1*$^{-/-}$ DN retina (see above). In addition, removing *Foxg1* from the chiasm reduced the growth of DN *Foxg1*$^{+/\pm}$ and *Foxg1*$^{-/-}$ retinal axons to levels below those of DN *Foxg1*$^{+/\pm}$ and *Foxg1*$^{-/-}$ retinal axons grown without chiasm cells, suggesting that the failure of many DN axons to penetrate the chiasm and instead to enter the ipsilateral optic tract in *Foxg1*$^{-/-}$ mutant mice might be explained by a chiasmatic defect.

Outgrowth of VT retinal axons on chiasm cells

As Foxg1 is not normally expressed in VT retina, we predicted that outgrowth from VT retina on chiasm cells might be unaffected by loss of Foxg1. Co-cultures were prepared in the following combinations: (1) VT *Foxg1*$^{+/\pm}$ retina ↔ *Foxg1*$^{+/\pm}$ chiasm; (2) VT *Foxg1*$^{-/-}$ retina ↔ *Foxg1*$^{+/\pm}$ chiasm; (3) VT *Foxg1*$^{+/\pm}$ retina ↔ *Foxg1*$^{-/-}$ chiasm; (4) VT *Foxg1*$^{-/-}$ retina ↔ *Foxg1*$^{-/-}$ chiasm. Previous work has shown that, in the presence of chiasm cells, wild-type VT retinal axons are shorter and fewer in number compared with axons from wild-type DN retina, reflecting the fact that many are repelled from the chiasm into the ipsilateral optic tract in vivo (Herrera et al., 2003; Herrera et al., 2004; Marcus et al., 1995; Marcus and Mason, 1995; Marcus et al., 1996; Wang et al., 1995). We observed the same result: values for percentage axon coverage and neurite length from VT retinae grown with chiasm cells were much lower (66-93% less) than from DN retinae grown with chiasm cells and from VT retinae grown without chiasm cells (compare values in Figs 5-7). Analysis of variance (ANOVA) indicated that, unlike data from the DN retinal co-cultures, there was no statistically significant effect of varying the genotype of the retina or the chiasm across the four co-culture combinations shown in Fig. 7A-F. Our data provide no evidence for a defect in the ability of *Foxg1*$^{-/-}$ VT RGC axons to grow on chiasm cells.

DISCUSSION

Our findings demonstrate a requirement for *Foxg1* in both DN retina and optic chiasm for the contralateral guidance of DN retinal axons at the ventral midline. Mice lacking Foxg1 have an abnormally elongated retina (Huh et al., 1999) but, despite this, mutant retina retains a normal volume and a normal number of RGCs (Pratt et al., 2004). We investigated the molecular changes in the retina underlying the increased ipsilateral routing of RGC axons in *Foxg1*$^{-/-}$ embryos and found a significant increase in the number of nasal RGCs expressing the ipsilateral determinant Zic2. RGCs expressing *Ephb1* were also found in nasal retina and are most probably responsible for the increased ipsilateral routing of *Foxg1*$^{-/-}$ nasal retinal axons owing to repulsion by ephrin B2 at the chiasm (Williams et al., 2003). Together, these findings suggest that: (1) *Foxg1*-expressing nasal retina is competent to express a genetic program, including the ipsilateral determinants Zic2 and EphB1, which are normally expressed only in Foxg1-negative VTC cells as their axons navigate the chiasm; and (2) Foxg1 normally represses this ipsilateral program within nasal RGCs to prevent the ipsilateral routing of their axons.

Patterning the retina

Previous descriptions have considered that the normal expression of *Foxg1* is limited mainly to nasal retina before and at the age when retinal axons are navigating the chiasm (Pratt et al., 2004; Hatini et al., 1994; Huh et al., 1999). Data presented here indicate a slight modification: the boundary of expression runs at an angle to the dorsoventral axis of the retina so that the expression domain of *Foxg1* is centred in DN retina. This means that the *Foxg1*-positive domain is complementary to the domain of expression of the
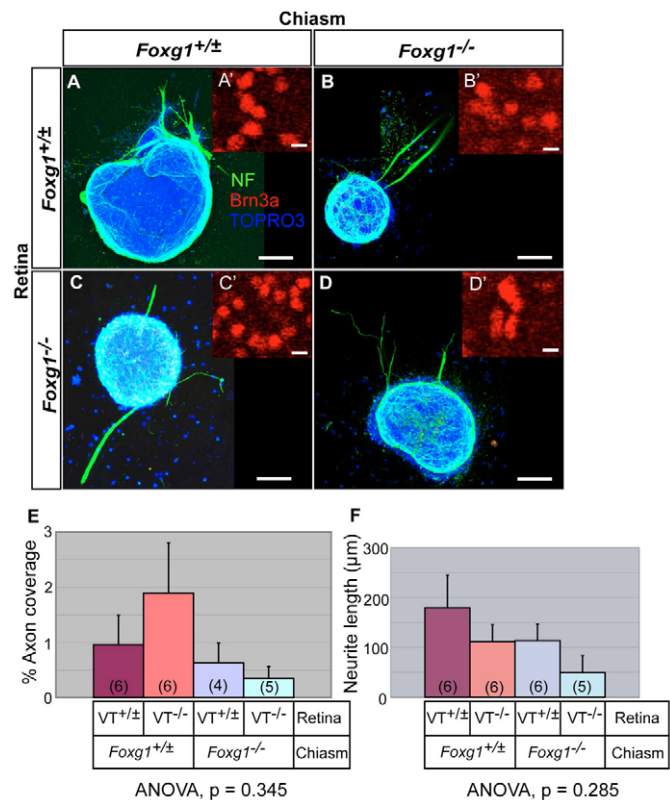
Fig. 7. Loss of Foxg1 from retina or chiasm has no significant effect on outgrowth of ventrotemporal retinal axons on chiasm cells in culture. (**A-D**) Co-cultures of *Foxg1*$^{+/\pm}$ or *Foxg1*$^{-/-}$ ventrotemporal (VT) retinal explants with dissociated *Foxg1*$^{+/\pm}$ or *Foxg1*$^{-/-}$ chiasm cells; immunohistochemistry and counterstaining are as in Fig. 6. (**A'-D'**) Brn3a expression in co-cultures A-D, respectively. (**E,F**) Mean percentage of axon coverage (±s.e.m.) 45 μm from the retinal explant (E) and mean lengths of the five longest neurites (±s.e.m.) (F). One-way ANOVA revealed no significant differences in outgrowth among retinal explants. (E,F) Numbers of explants are in parentheses. Scale bars: 100 μm in A-D; 10 μm in A'-D'.

transcription factor *Foxd1*, which is centred in VT retina (Herrera et al., 2004). Previous studies have shown: (1) that loss of Foxd1 results in loss of Zic2 and EphB1 from the VTC, suggesting that Foxd1 is an upstream activator of *Zic2* and *Ephb1* (Herrera et al., 2004); and (2) that loss of Foxd1 results in an expansion of *Foxg1* into VT retina, suggesting that Foxd1 represses Foxg1 in the retina (Herrera et al., 2004). In light of our present findings indicating that Foxg1 represses Zic2 and EphB1, the loss of Zic2 and EphB1 expression in *Foxd1*$^{-/-}$ mutants might be explained by the expansion of Foxg1 into VT retina.

Could loss of Foxg1 cause an upregulation of Zic2 and EphB1 in DN retina via an ectopic DN expression of Foxd1? Our results suggest that this is possible, as *Foxd1* expression expands into the DN retina of *Foxg1*$^{-/-}$ mutants. Based on current evidence, there are several possibilities to explain the actions of Foxg1 and Foxd1 in the normal retina: (1) Foxd1 might be a direct upstream activator of *Zic2* and *Ephb1*, and Foxg1 might prevent *Zic2* and *Ephb1* expression in DN retina indirectly by preventing expression of Foxd1; (2) Foxg1 might be a direct upstream repressor of *Zic2* and *Ephb1*, and Foxd1 might allow expression of *Zic2* and *Ephb1* in VT retina indirectly by preventing

expression of Foxg1; (3) both Foxd1 and Foxg1 might be direct regulators (positive and negative, respectively) of *Zic2* and *Ephb1* expression.

In normal retina, the expression domains of Zic2 and EphB1 are restricted peripherally in VT retina to cells in the VTC that are in the process of forming permanent ipsilateral projections. Later, Zic2 is rapidly downregulated once these projections have formed, while EphB1 expression becomes more widespread in the retina, where it may regulate other processes (Herrera et al., 2003; Williams et al., 2003). We observed characteristically restricted expression of Zic2 and *Ephb1* not only in VT retina but also in DN retina of *Foxg1*$^{-/-}$ mutants, where ectopic expression of Zic2 and *Ephb1* was mainly in its peripheral region. This suggests that the sequence of events that generate ipsilateral projections from VT retina might also be followed in DN retina of *Foxg1*$^{-/-}$ mutants.

Foxg1 represses ipsilateral axon guidance from nasal retina

Our results indicate that *Foxg1* is required by DN retina for its axons to grow to their normal extent on chiasm cells in vitro and hence for them to penetrate the chiasm to grow contralaterally in normal numbers in vivo. This might occur because Foxg1 normally represses expression of an ipsilateral determinant in DN retina or activates expression of a contralateral determinant in DN retina. Our evidence supports the former by revealing a significant increase in Zic2- and *Ephb1*-expressing cells in *Foxg1*$^{-/-}$ nasal retina. In the VTC, expression of Zic2 by RGCs is sufficient for their axons to project ipsilaterally (Herrera et al., 2003). Our findings suggest that abnormal expression of Zic2 by RGCs in DN retina can also redirect their axons ipsilaterally. This is in excellent agreement with recently reported findings by Garcia-Frigola et al. (Garcia-Frigola et al., 2008), who showed that misexpression of Zic2 in RGCs outside the VTC during a specific time-window around E13.5 is sufficient to direct the axons of those RGCs ipsilaterally. In E14.5 and E16.5 *Foxg1*$^{-/-}$ embryos, we found seven- to eightfold increases in numbers of Zic2-expressing cells in DN retina, very close to the eightfold increases in ipsilateral projections reported previously in E15.5 *Foxg1*$^{-/-}$ embryos (Pratt et al., 2004). In the normal VTC, Zic2 is thought to act via positive transcriptional regulation of the EphB1 axon guidance receptor (Williams et al., 2003; Herrera et al., 2003; Lee at al., 2008; Garcia-Frigola et al., 2008) and our results suggest that this same mechanism occurs in the DN retina in the absence of Foxg1. Our results indicate that DN cells are competent to express an ipsilateral program characteristic of the VTC in the absence of Foxg1 protein.

A likely model is that Foxg1 in DN retina normally represses *Zic2*; thus, reducing expression of its downstream target *Ephb1* and preventing repulsive EphB1-ephrin B2 interactions between retinal axons and chiasm cells, although a parallel direct effect of Foxg1 on *Ephb1* expression can not be excluded. Other hypotheses are possible but less attractive. Previous findings have identified a link between the contralateral projection and the transcription factor islet 2 (Pak et al., 2004) and cell-adhesion molecule Nr-CAM (Williams et al., 2006). Both islet 2 and Nr-CAM are expressed in contralaterally projecting RGCs and mice lacking these genes display an increased ipsilateral projection. However, these abnormal projections arise from RGCs confined to the VTC and, in the case of Nr-CAM mutants, are generated later than the abnormal ipsilateral projections in *Foxg1*$^{-/-}$ embryos (Pak et al., 2004; Williams et al., 2006). It seems probable, therefore, that any loss of islet 2 or Nr-CAM in *Foxg1*$^{-/-}$ retinae would not explain in a simple way the respecification of normally contralaterally projecting nasal RGCs to an ipsilateral fate, as observed in *Foxg1*$^{-/-}$ embryos (Pratt et al., 2004).

Foxg1 controls axon guidance at the chiasm

The extra ipsilateral projections in *Foxg1*$^{-/-}$ embryos arise from temporal as well as nasal RGCs (Pratt et al., 2004). The greatest increases in numbers of Zic2-expressing cells were confined to nasal retina, where Foxg1 is normally expressed, with only a small but significant increase in dorsotemporal (DT) retina at E16.5, which is too late to explain the increased ipsilateral projection from the temporal retina of *Foxg1*$^{-/-}$ embryos. This increased projection from temporal retina is probably caused by defects at the optic chiasm. This might be due to changes in the biochemistry of chiasm cells or might arise as a secondary consequence of the altered routing of a large proportion of axons from the nasal retina.

Our studies provide direct evidence that, in addition to its action in the retina, Foxg1 also functions as a contralateral determinant by regulating the environment at the chiasm. Our culture work indicated that *Foxg1*$^{-/-}$ chiasm cells are less supportive than *Foxg1*$^{+/+}$ chiasm cells of retinal axons growing across them. Current hypotheses on the mechanisms guiding the laterality of RGC axons at the chiasm focus on the importance of inhibitory interactions that repel some axons into the ipsilateral tract (Nakagawa et al., 2000; Williams et al., 2003). On the other hand, our findings indicated that DN axons grow better in the presence of chiasm cells than in their absence, suggesting that chiasm cells might play an active role supporting the growth of DN axons across them. Interestingly, previous studies using a similar culture approach found no such evidence for a growth-promoting effect of chiasm cells on DN axons; in some cases, the presence of chiasm cells inhibited the growth of DN axons (Wang et al., 1995; Williams et al., 2003; Williams et al., 2006). There are several differences between the methods we used and those of others. A potentially crucial difference is that, unlike previous workers, we placed chiasm cells in a collagen gel rather than on a laminin substrate. Previous work has shown that laminin can convert growth cone attraction to growth cone repulsion (Hopker et al., 1999); it is possible that our results are explained by the release of a growth-promoting molecule whose actions are reversed or negated depending on the substrate used.

Loss of Foxg1 from chiasm cells removes their ability to support the growth of Foxg1-expressing DN axons. One possible explanation for this is that Foxg1 at the chiasm normally upregulates the expression of growth-promoting molecules. Alternatively, or in addition, Foxg1 at the chiasm might prevent the expression of growth-inhibiting molecules, and/or modifiers of those inhibitory molecules, that might otherwise counteract the growth promoting activity of chiasm cells. Evidence that the second possible mechanism contributes to the net action of Foxg1 comes from our finding that there is less outgrowth from retinal explants grown on chiasm cells lacking Foxg1 than from chiasm cells cultured with no chiasm cells. Given the potential complexity of the effects of Foxg1 at the chiasm and the fact that previous work has not shown changes in the expression of obvious candidate molecules, including ephrin B2, CD44, SSEA-1 (Pratt et al., 2004) and Zic2 (N.M.T., T.P. and D.J.P., unpublished), a systematic unbiased approach to identifying molecular changes at the chiasm in the absence of Foxg1 is now indicated.

Supplementary material

Supplementary material for this article is available at
http://dev.biologists.org/cgi/content/full/135/24/4081/DC1

References

Brown, L. Y., Kottmann, A. H. and Brown, S. (2003). Immunolocalization of Zic2 expression in the developing mouse forebrain. *Gene Expr. Patterns* **3**, 361-367.

Christoffels, V. M., Keijser, A. G., Houweling, A. C., Clout, D. E. and Moorman, A. F. (2000). Patterning the embryonic heart: identification of five mouse Iroquois homeobox genes in the developing heart. *Dev. Biol.* **224**, 263-274.

Chung, K. Y., Shum, D. K. and Chan, S. O. (2000a). Expression of chondroitin sulfate proteoglycans in the chiasm of mouse embryos. *J. Comp. Neurol.* **417**, 153-163.

Chung, K. Y., Taylor, J. S., Shum, D. K. and Chan, S. O. (2000b). Axon routing at the optic chiasm after enzymatic removal of chondroitin sulfate in mouse embryos. *Development* **127**, 2673-2683.

Colello, R. J. and Guillery, R. W. (1990). The early development of retinal ganglion cells with uncrossed axons in the mouse: retinal position and axonal course. *Development* **108**, 515-523.

Drager, U. C. (1985). Birth dates of retinal ganglion cells giving rise to the crossed and uncrossed optic projections in the mouse. *Proc. R. Soc. Lond. B Biol. Sci.* **224**, 57-77.

Drager, U. C. and Olsen, J. F. (1980). Origins of crossed and uncrossed retinal projections in pigmented and albino mice. *J. Comp. Neurol.* **191**, 383-412.

Erskine, L. and Herrera, E. (2007). The retinal ganglion cell axon's journey: insights into molecular mechanisms of axon guidance. *Dev. Biol.* **308**, 1-14.

Erskine, L., Williams, S. E., Brose, K., Kidd, T., Rachel, R. A., Goodman, C. S., Tessier-Lavigne, M. and Mason, C. A. (2000). Retinal ganglion cell axon guidance in the mouse optic chiasm: expression and function of robos and slits. *J. Neurosci.* **20**, 4975-4982.

Garcia-Frigola, C., Carreres, M. I., Vegar, C., Mason, C. and Herrera, E. (2008). Zic2 promotes axonal divergence at the optic chiasm midline by EphB1-dependent and -independent mechanisms. *Development* **135**, 1833-1841.

Guillery, R. W., Mason, C. A. and Taylor, J. S. (1995). Developmental determinants at the mammalian optic chiasm. *J. Neurosci.* **15**, 4727-4737.

Hatini, V., Tao, W. and Lai, E. (1994). Expression of winged helix genes, BF-1 and BF-2, define adjacent domains within the developing forebrain and retina. *J. Neurobiol.* **25**, 1293-1309.

Hebert, J. M. and McConnell, S. K. (2000). Targeting of cre to the Foxg1 (BF-1) locus mediates loxP recombination in the telencephalon and other developing head structures. *Dev. Biol.* **222**, 296-306.

Herrera, E., Brown, L., Aruga, J., Rachel, R. A., Dolen, G., Mikoshiba, K., Brown, S. and Mason, C. A. (2003). Zic2 patterns binocular vision by specifying the uncrossed retinal projection. *Cell* **114**, 545-557.

Herrera, E., Marcus, R., Li, S., Williams, S. E., Erskine, L., Lai, E. and Mason, C. (2004). Foxd1 is required for proper formation of the optic chiasm. *Development* **131**, 5727-5739.

Hopker, V. H., Shewan, D., Tessier-Lavigne, M., Poo, M. and Holt, C. E. (1999). Growth-cone attraction to netrin-1 is converted to repulsion by laminin-1. *Nature* **401**, 69-73.

Huh, S., Hatini, V., Marcus, R. C., Li, S. C. and Lai, E. (1999). Dorsal-ventral patterning defects in the eye of BF-1-deficient mice associated with a restricted loss of shh expression. *Dev. Biol.* **211**, 53-63.

Insausti, R., Blakemore, C. and Cowan, W. M. (1984). Ganglion cell death during development of ipsilateral retino-collicular projection in golden hamster. *Nature* **308**, 362-365.

Lee, R., Petros, T. J. and Mason, C. A. (2008). Zic2 regulates retinal ganglion cell axon avoidance of ephrinB2 through inducing expression of the guidance receptor EphB1. *J. Neurosci.* **28**, 5910-5919.

Marcus, R. C. and Mason, C. A. (1995). The first retinal axon growth in the mouse optic chiasm: axon patterning and the cellular environment. *J. Neurosci.* **15**, 6389-6402.

Marcus, R. C., Blazeski, R., Godement, P. and Mason, C. A. (1995). Retinal axon divergence in the optic chiasm: uncrossed axons diverge from crossed axons within a midline glial specialization. *J. Neurosci.* **15**, 3716-3729.

Marcus, R. C., Wang, L. C. and Mason, C. A. (1996). Retinal axon divergence in the optic chiasm: midline cells are unaffected by the albino mutation. *Development* **122**, 859-868.

Mason, C. A. and Sretavan, D. W. (1997). Glia, neurons, and axon pathfinding during optic chiasm development. *Curr. Opin. Neurobiol.* **7**, 647-653.

Nakagawa, S., Brennan, C., Johnson, K. G., Shewan, D., Harris, W. A. and Holt, C. E. (2000). Ephrin-B regulates the Ipsilateral routing of retinal axons at the optic chiasm. *Neuron* **25**, 599-610.

Niclou, S. P., Jia, L. and Raper, J. A. (2000). Slit2 is a repellent for retinal ganglion cell axons. *J. Neurosci.* **20**, 4962-4974.

Pak, W., Hindges, R., Lim, Y. S., Pfaff, S. L. and O'Leary, D. D. (2004). Magnitude of binocular vision controlled by islet-2 repression of a genetic program that specifies laterality of retinal axon pathfinding. *Cell* **119**, 567-578.

Pan, L., Yang, Z., Feng, L. and Gan, L. (2005). Functional equivalence of Brn3 POU-domain transcription factors in mouse retinal neurogenesis. *Development* **132**, 703-712.

Plump, A. S., Erskine, L., Sabatier, C., Brose, K., Epstein, C. J., Goodman, C. S., Mason, C. A. and Tessier-Lavigne, M. (2002). Slit1 and Slit2 cooperate to prevent premature midline crossing of retinal axons in the mouse visual system. *Neuron* **33**, 219-232.

Pratt, T., Tian, N. M., Simpson, T. I., Mason, J. O. and Price, D. J. (2004). The winged helix transcription factor Foxg1 facilitates retinal ganglion cell axon crossing of the ventral midline in the mouse. *Development* **131**, 3773-3784.

Pratt, T., Conway, C. D., Tian, N. M., Price, D. J. and Mason, J. O. (2006). Heparan sulphation patterns generated by specific heparan sulfotransferase enzymes direct distinct aspects of retinal axon guidance at the optic chiasm. *J. Neurosci.* **26**, 6911-6923.

Ringstedt, T., Braisted, J. E., Brose, K., Kidd, T., Goodman, C., Tessier-Lavigne, M. and O'Leary, D. D. (2000). Slit inhibition of retinal axon growth and its role in retinal axon pathfinding and innervation patterns in the diencephalon. *J. Neurosci.* **20**, 4983-4991.

Sretavan, D. W., Feng, L., Pure, E. and Reichardt, L. F. (1994). Embryonic neurons of the developing optic chiasm express L1 and CD44, cell surface molecules with opposing effects on retinal axon growth. *Neuron* **12**, 957-975.

Sretavan, D. W., Pure, E., Siegel, M. W. and Reichardt, L. F. (1995). Disruption of retinal axon ingrowth by ablation of embryonic mouse optic chiasm neurons. *Science* **269**, 98-101.

Thompson, H., Barker, D., Camand, O. and Erskine, L. (2006a). Slits contribute to the guidance of retinal ganglion cell axons in the mammalian optic tract. *Dev. Biol.* **296**, 476-484.

Thompson, H., Camand, O., Barker, D. and Erskine, L. (2006b). Slit proteins regulate distinct aspects of retinal ganglion cell axon guidance within dorsal and ventral retina. *J. Neurosci.* **26**, 8082-8091.

Tuttle, R., Braisted, J. E., Richards, L. J. and O'Leary, D. D. (1998). Retinal axon guidance by region-specific cues in diencephalon. *Development* **125**, 791-801.

Wang, L. C., Dani, J., Godement, P., Marcus, R. C. and Mason, C. A. (1995). Crossed and uncrossed retinal axons respond differently to cells of the optic chiasm midline *in vitro*. *Neuron* **15**, 1349-1364.

Wang, L. C., Rachel, R. A., Marcus, R. C. and Mason, C. A. (1996). Chemosuppression of retinal axon growth by the mouse optic chiasm. *Neuron* **17**, 849-862.

Williams, S. E., Mann, F., Erskine, L., Sakurai, T., Wei, S., Rossi, D. J., Gale, N. W., Holt, C. E., Mason, C. A. and Henkemeyer, M. (2003). Ephrin-B2 and EphB1 mediate retinal axon divergence at the optic chiasm. *Neuron* **39**, 919-935.

Williams, S. E., Grumet, M., Colman, D. R., Henkemeyer, M., Mason, C. A. and Sakurai, T. (2006). A role for Nr-CAM in the patterning of binocular visual pathways. *Neuron* **50**, 535-547.

Xuan, S., Baptista, C. A., Balas, G., Tao, W., Soares, V. C. and Lai, E. (1995). Winged helix transcription factor BF-1 is essential for the development of the cerebral hemispheres. *Neuron* **14**, 1141-1152.